

How Do Nonlinear Voids Affect Light Propagation ?

Norimasa SUGIURA^{1,*} Ken-ichi NAKAO^{2,**} Daisuke IDA^{1,***} Nobuyuki
SAKAI^{3,****} and Hideki ISHIHARA^{4,*****}

¹*Department of Physics, Kyoto University, Kyoto 606-8502, Japan*

²*Department of Physics, Osaka City University, Osaka 558-8585, Japan*

³*Yukawa Institute for Theoretical Physics, Kyoto University
Kyoto 606-8502, Japan*

⁴*Department of Physics, Tokyo Institute of Technology
Tokyo 152-0033, Japan*

(Received September 29, 1999)

Propagation of light in a clumpy universe is examined. As an inhomogeneous matter distribution, we take a spherical void surrounded by a dust shell, where the “lost mass” in the void is compensated by the shell. We study how the angular-diameter distance behaves when such a structure exists. The angular-diameter distance is calculated by integrating the Raychaudhuri equation including the shear. An explicit expression for the junction condition for the massive thin shell is calculated. We apply these results to a dust shell embedded in a Friedmann universe and determine how the distance-redshift relation is modified compared with that in the purely Friedmann universe. We also study the distribution of distances in a universe filled with voids. We show that the void-filled universe gives a larger distance than the FRW universe by $\sim 5\%$ at $z \sim 1$ if the size of the void is $\sim 5\%$ of the Horizon radius.

§1. Introduction

One of the most interesting findings of the nearby redshift surveys is the discovery of large voids and that they appear to be a common feature of galaxy distributions. Great interest in such voids was first aroused by the discovery of the Boötes void,¹⁾ which was confirmed to have a radius of $\sim 60 h^{-1}\text{Mpc}$.²⁾ At that stage, however, it could not be concluded that voids are common structures in the universe. The idea that voids are in fact common features of the large-scale structure of our universe was established by the recent surveys beginning from the CfA redshift survey,³⁾ which introduced a picture of the universe where the galaxies are located on the surfaces of bubble-like structures with diameters 25 – 50 Mpc. Using the survey data such as CfA2⁴⁾ and SSRS2,⁵⁾ El-Ad *et al.*,⁶⁾ who established a method to find voids in these galaxy distributions, revealed that a substantial fraction of the volume of our universe is occupied by underdensity regions; they have shown that about half of the volume is filled with voids and that the voids have a diameter of at least $40h^{-1}\text{Mpc}$ with an average underdensity of -0.9 .

*) E-mail: sugiura@tap.scphys.kyoto-u.ac.jp

**) E-mail: knakao@sci.osaka-cu.ac.jp

***) E-mail: ida@tap.scphys.kyoto-u.ac.jp

****) E-mail: sakai@yukawa.kyoto-u.ac.jp

*****) E-mail: ishihara@th.phys.titech.ac.jp

With the motivation of explaining such large voids, the gravitational evolution of a less-dense region has been studied by several authors.^{7), 8)} It was shown⁸⁾ that a less-dense region expands faster than the outer region, and a dense thin shell is formed behind the shock front by the “snow-plow” mechanism. The general relativistic motion of the void’s shell was also studied by Maeda and Sato.⁹⁾ They adopted the metric junction method developed by Israel¹⁰⁾ and derived an expansion law of a void in the Friedmann-Robertson-Walker (FRW) universe. In addition to these, non-gravitational scenarios for the formation of voids have also been proposed. For example, in the explosion model,¹¹⁾ a void surrounded by a thin shell is formed by the explosion of a pregalactic object. Another example is given by an inflationary model with a first-order phase transition, where vacuum bubbles are nucleated during inflation. These bubbles could represent the origin of voids.¹²⁾ Thus the void model not only provides a simple picture of nonlinear density fluctuations but also is supported by many observational and theoretical considerations.

There are also studies which investigate light propagation properties in a void system, such as the observational effect of voids on CMB anisotropies and the modification of the redshift and luminosity for distant sources due to the existence of voids. The effects on the CMB anisotropies were discussed by several authors,^{13), 14)} suggesting that further CMB observations will give some constraints on the configuration and origin of voids. Investigation of the light propagation properties in a clumpy universe using a spherical void model was undertaken by Sato,¹⁵⁾ who discussed the modification of the redshift and luminosity in comparison with the FRW model. He found that the modification is third order in (Hr_v/c) for the redshift and first order in (Hr_v/c) for the luminosity, where H is the Hubble parameter, r_v is the size of the void and c is the velocity of light. We believe, however, his result is suspect because the condition for the distance junction he adopted seems to be inappropriate.

In this paper, we study light propagation in a void system based on the Raychaudhuri equation. A light ray bundle traveling across a spherical void surrounded by a thin shell suffers (de-)magnification and shear focusing. We calculate the modification of the distance and redshift in comparison with the FRW model. Light propagation in the Swiss Cheese model has been studied extensively,^{16), 17)} but studies on a void surrounded by an overdense shell are far from complete. This paper gives an exact treatment of such a system.

The organization of this paper is as follows. In §2 we derive the junction condition for the expansion and shear of a null ray bundle across a shell. In §3 we calculate the modification of the distance and the redshift caused by the void-shell system and discuss its cosmological implications. The last section is devoted to a summary. We follow the signature of the metric and the convention of the Riemann tensor used in Ref. 18).

§2. Basic equations

In this paper, we consider a spherical void in the FRW universe. We assume that the interior of the void is a vacuum, so that the spacetime inside the void is

flat. The mass that would have been in the void is assumed to be distributed in a spherical shell surrounding the void. We treat the matter in the shell as an infinitely thin dust shell.

In this section, we derive an expression for the angular-diameter distance in a flat spacetime and in FRW spacetime, which respectively correspond to the inside and outside spacetime of the void. We also derive the junction condition for the expansion and shear of a light ray bundle across the dust shell.

2.1. Basic relations in geometric optics

We use the notation used by Sasaki.¹⁹⁾ Let k^a be the tangent of a null geodesic parameterized by an affine parameter, λ . We introduce a null vector field, l^a , defined by

$$l^a l_a = 0, \quad l^a k_a = -1, \quad l^a{}_{;b} k^b = 0, \quad (2.1)$$

where the semi-colon denotes the covariant derivative. Using these vectors, we define the metric H_{ab} on the two-dimensional screen placed orthogonal to the spatial direction of the null geodesics:

$$H_{ab} \equiv g_{ab} + k_a l_b + l_a k_b. \quad (2.2)$$

The expansion θ and the shear σ of the cross section of the beam are defined by

$$\theta = k^a{}_{;a}, \quad \sigma_{ab} = H_a{}^c \left(k_{c;d} - k_{d;c} - \frac{1}{2} H_{cd} \right) H_b{}^d. \quad (2.3)$$

We also introduce a dyad, $\{e_A^a\}$ ($A = 1, 2$), on the screen such that

$$H_{ab} = \delta_{AB} e_a{}^A e_b{}^B, \quad g^{ab} e_a{}^A e_b{}^B = H^{AB} e_a{}^A e_b{}^B = \delta^{AB} \quad \text{and} \quad e_{A;b}^a k^b = 0; \quad (2.4)$$

i.e. they are parallel-propagated along the geodesics. Then the basic equations of the geometric optics can be written as²⁰⁾

$$\frac{d\theta}{d\lambda} = -R_{44} - \sigma^{AB} \sigma_{AB} - \frac{1}{2} \theta^2, \quad (2.5)$$

$$\frac{d\sigma_{AB}}{d\lambda} = -C_{A4B4} - \theta \sigma_{AB}, \quad (2.6)$$

with

$$\sigma_{AB} = \sigma_{ab} e_A^a e_B^b, \quad R_{44} \equiv R_{ab} k^a k^b, \quad C_{A4B4} \equiv C_{abcd} e_A^a k^b e_B^c k^d, \quad (2.7)$$

where R_{ab} and C_{abcd} are the Ricci and Weyl tensor, respectively. Finally, we define the angular-diameter distance d_A by

$$\frac{d}{d\lambda} \ln d_A = \frac{1}{2} \theta. \quad (2.8)$$

By integrating Eqs. (2.5), (2.6) and (2.8), we can obtain the angular-diameter distance. We can also write the equation for d_A as

$$\frac{d^2}{d\lambda^2} d_A / d_A = -\frac{1}{2} R_{44} - \frac{1}{2} \sigma^{AB} \sigma_{AB}. \quad (2.9)$$

This expression is especially useful when the shear term vanishes.

2.2. Inside the void—flat spacetime

In flat spacetime, the Raychaudhuri equations reduce to

$$\frac{d}{d\lambda}\theta = -\frac{1}{2}\theta^2 - \sigma^{AB}\sigma_{AB} \quad (2.10)$$

and

$$\frac{d}{d\lambda}\sigma_{AB} = -\theta\sigma_{AB}. \quad (2.11)$$

Suppose that the expansion θ is positive initially, which implies that the derivative of d_A is positive. Then the angular diameter-distance is given by

$$d_A = d_{A0} \left\{ 1 + \frac{1}{2}\theta_0(\lambda - \lambda_0) \right\} \sqrt{1 - \left\{ \frac{|\sigma_{AB0}|(\lambda - \lambda_0)}{1 + \frac{1}{2}\theta_0(\lambda - \lambda_0)} \right\}^2}, \quad (2.12)$$

where $|\sigma_{AB0}| \equiv |\sigma_{AB0}\sigma_0^{AB}|^{1/2}$. Note that when the shear vanishes, the distance is proportional to the time coordinate:

$$\frac{d}{dt}d_A = \text{constant}. \quad (2.13)$$

By inspecting Eq. (2.12), one can see that the shear term appears as a correction to the shear-free case.

2.3. Jumps of the optical scalars across the singular hypersurface

The shell which surrounds the void generates a timelike hypersurface through its motion. Since we treat the shell as infinitely thin, the hypersurface may be regarded as singular. We follow the procedure to treat a singular hypersurface formulated by Israel.¹⁰⁾ In order to obtain the jumps of the expansion and the shear of a null geodesic bundle across the shell, we proceed as follows.

We consider a spacetime V with a timelike singular hypersurface Σ . The singular hypersurface Σ divides V into two regions, V_+ and V_- . Consider a field variable Ψ defined on Σ . The values of Ψ evaluated on either side of Σ will be denoted by Ψ_{\pm} and the jump is defined by

$$[\Psi] \equiv \Psi_+ - \Psi_-. \quad (2.14)$$

We introduce a spacelike unit vector field n^a ($n^a n_a = +1$) normal to Σ and the projection operator $h_b^a \equiv \delta_b^a - n^a n_b$. The extrinsic curvature K_{ab} is then given by

$$K_{ab} = -\frac{1}{2}h_a^c h_b^d \mathcal{L}_n h_{cd} = -h_a^c h_b^d \nabla_c n_d, \quad (2.15)$$

where \mathcal{L}_n and ∇_a are the Lie derivative along n^a and the covariant derivative, respectively. We have two extrinsic curvatures, $K_{ab}|_{\pm}$, which may differ, since Σ is singular. The jump of K_{ab} across Σ can be written in the form

$$[K_{ab}] = 8\pi G \left(S_{ab} - \frac{1}{2}h_{ab}S_c^c \right). \quad (2.16)$$

The tensor S_{ab} here is related to the stress-energy tensor T_{ab} through the equation

$$S_{ab} = \lim_{\epsilon \rightarrow 0} \int_{-\epsilon}^{+\epsilon} T_{cd} h_a^c h_b^d dx, \quad (2.17)$$

where x is a Gaussian normal coordinate ($x = 0$ on Σ). Hence S_{ab} is regarded as the surface stress-energy tensor of Σ .

The jumps of θ and σ_{AB} on Σ are calculated by integrating Eqs.(2.5) and (2.6) as

$$[\theta] = - \lim_{\epsilon \rightarrow 0^+} \int_{-\epsilon}^{+\epsilon} R_{44} dx/k^n, \quad (2.18)$$

$$[\sigma_{AB}] = - \lim_{\epsilon \rightarrow 0^+} \int_{-\epsilon}^{+\epsilon} C_{A4B4} dx/k^n, \quad (2.19)$$

where

$$k^n \equiv k^a n_a. \quad (2.20)$$

Here we have set n^a to point in the direction in which the affine parameter increases. From the above equations, we see that the jumps of θ and σ_{AB} on Σ come from the diverging parts of R_{44} and C_{A4B4} on Σ . Thus our next task is to calculate R_{44} and C_{A4B4} . After a straightforward manipulation, we find

$$R_{44} = (k^n)^2 \mathcal{L}_n K_c^c + k^a k^b h_a^c h_b^d \mathcal{L}_n K_{cd} + \text{finite term}, \quad (2.21)$$

$$C_{A4B4} = \left\{ \left(e_A^n e_B^n - \frac{1}{2} \delta_{AB} \right) k^a k^b - k^n (e_A^n e_B^a + e_B^n e_A^a) k^b + (k^n)^2 e_A^a e_B^b \right\} \\ \times h_a^c h_b^d \mathcal{L}_n K_{cd} - \frac{1}{2} \delta_{AB} (k^n)^2 \mathcal{L}_n K_c^c + \text{finite term}, \quad (2.22)$$

where $e_A^n \equiv e_A^a n_a$. Using Eqs. (2.16) and (2.18)–(2.22), we finally obtain the jumps of θ and σ_{AB} as

$$[\theta] = - \frac{8\pi G}{k^n} k^a k^b S_{ab}, \quad (2.23)$$

$$[\sigma_{AB}] = - \frac{8\pi G}{k^n} \left\{ \left(e_A^n e_B^n - \frac{1}{2} \delta_{AB} \right) k^a k^b - k^n (e_A^n e_B^a + e_B^n e_A^a) k^b + (k^n)^2 e_A^a e_B^b \right\} \\ \times \left(S_{ab} - \frac{1}{2} h_{ab} S_c^c \right) - 2\pi G \delta_{AB} k^n S_c^c. \quad (2.24)$$

In this paper, we assume that the singular hypersurface which approximates the wall of the void has a surface stress-energy tensor of the dust type (we call it a dust shell),

$$S_{ab} = D u_a u_b, \quad (2.25)$$

where D is the surface density and u^a is the 4-velocity of the shell ($u^a u_a = -1$). In the case of the dust shell, Eqs. (2.23) and (2.24) become

$$[\theta] = - \frac{8\pi G}{k^n} D (k^u)^2, \quad (2.26)$$

$$[\sigma_{AB}] = -\frac{4\pi G}{k^n} D \left[2(e_A^n k^u - e_A^u k^n)(e_B^n k^u - e_B^u k^n) + \delta_{AB} \left\{ (k^n)^2 - (k^u)^2 \right\} \right], \quad (2.27)$$

where

$$k^u \equiv k^a u_a \quad \text{and} \quad e_A^u \equiv e_A^a u_a. \quad (2.28)$$

2.4. Outside the void—FRW spacetime

We note here the analytical expression for the distance-redshift relation in flat FRW spacetime. The basic assumption is that the shear is negligible. We find the expression for d_A in terms of the cosmic time t as

$$d_A = d_{Ai} \left\{ 3 \left(\frac{t}{t_i} \right)^{2/3} - 2 \left(\frac{t}{t_i} \right) \right\} + \frac{t_i}{2k_i} d_{Ai} \theta_i \left\{ 3 \left(\frac{t}{t_i} \right) - 3 \left(\frac{t}{t_i} \right)^{2/3} \right\}, \quad (2.29)$$

with an appropriate boundary condition for θ_i , where k_i is the frequency of the ray observed by a comoving observer at $t = t_i$.

§3. Application and discussion

3.1. Single void

We consider a spherical void surrounded by a dust shell in a flat FRW universe (which we refer to in the following as a “FRW model”). The matter that would have been inside the void is distributed in the shell and we assume that the external universe is undisturbed. This is exactly the same as the model analyzed by Thompson and Vishniac.¹³⁾ We consider a light ray bundle traveling across the void and calculate the redshift and the angular-diameter distance using the junction conditions obtained in the previous section. The result will be compared with the FRW relation.

The metric of the FRW model is given by

$$ds^2 = -dt^2 + a(t)^2(dr^2 + r^2 d\Omega^2). \quad (3.1)$$

The void is an empty region which can be described by a flat metric,

$$ds^2 = -dt'^2 + dx'^2 + x'^2 d\Omega^2, \quad (3.2)$$

where the primes denote internal coordinates. The coordinate radius of the void is $r_v(t)$ in the external coordinates and $x'_v(t')$ in the internal coordinates. They must satisfy

$$x'_v(t) = a(t)r_v(t). \quad (3.3)$$

Maeda and Sato⁹⁾ and Bertschinger²¹⁾ showed that the shell radius expands asymptotically as

$$r_v(t) \propto t^\beta \quad \text{with} \quad \beta \sim 0.13. \quad (3.4)$$

In the following, the subscripts 1 and 2, respectively, denote quantities at the time the photon enters the void and at the time it leaves. Primes denote quantities measured by an observer at rest in the internal coordinate system, and unprimed quantities are measured by an observer comoving in the universe just outside the shell of the void.

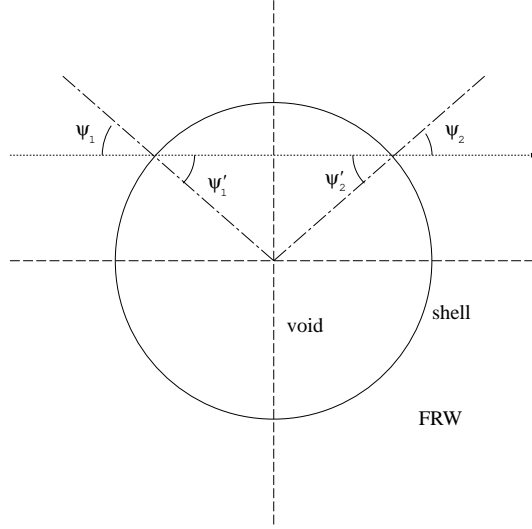


Fig. 1. Cross section of a void and the photon path through the $\phi = \pi/2$ plane. The expansion of the void is not shown explicitly.

The light ray bundle enters the void at $t = t_1$ (corresponding to $t' = t_1'$ in the internal coordinates). Then the light arrives at the other side of the void at $t = t_2$ ($t' = t_2'$). The arrival time is obtained by solving the equations

$$t_2' - t_1' = x_1' \cos \Psi_1' + x_2' \cos \Psi_2', \quad (3.5)$$

$$x_1' \sin \Psi_1' = x_2' \sin \Psi_2'. \quad (3.6)$$

(See Fig. 1 for the definition of the angular variables.) The redshift and the distance are obtained by solving the geodesic equation and the Raychaudhuri equations, as we do in the following. We also calculate the distance and redshift of a null ray in the FRW model which has traveled from t_1 to t_2 . We then compare the distances and redshifts for these two models (see Fig.2).

Just before entering the shell, the light ray bundle has k_1 , $d_A^- = d_{A1}$, θ_1 and $\sigma_{AB1} = 0$. At the time it crosses the shell, we impose Eq. (2.26) for θ , Eq. (2.27) for σ , and the following conditions for k and d_A :

$$k^a u_a = k^{a'} u_{a'}, \quad k^a n_a = k^{a'} n_{a'}, \quad d_A^+ = d_A^-. \quad (3.7)$$

Note that these conditions for k^a give the same result as that obtained by the Lorentz transformation adopted by Thompson and Vishniac.¹³⁾ From Eq. (2.12), the distance at the time the ray bundle leaves the void is given by

$$d_A(t_2') = d_{A1} \left\{ 1 + \frac{\theta_1'}{2k_1'} (t_2' - t_1') \right\} \times \{1 + \Delta\}, \quad (3.8)$$

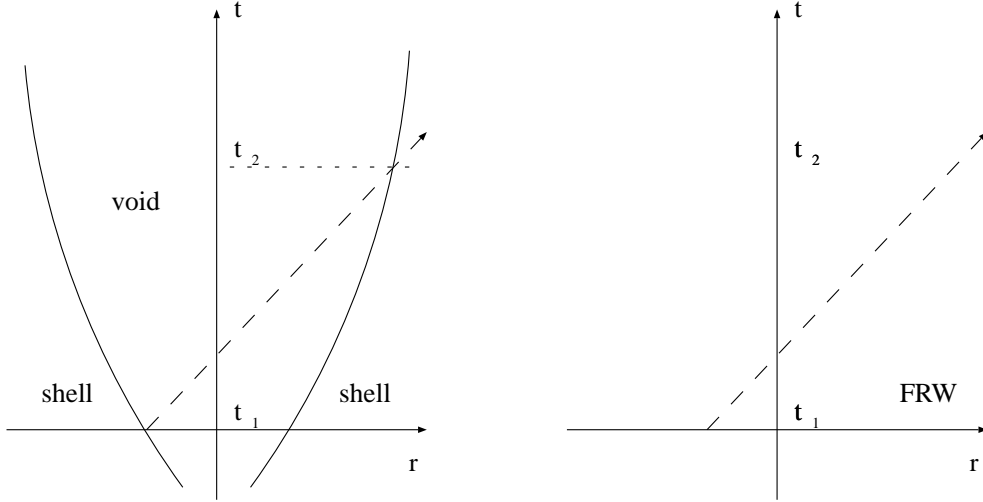


Fig. 2. Trajectory of a dust shell and the path of a light ray in the void-shell system (*left*). For comparison, we consider a light ray which travels in the FRW universe for the same time interval measured outside the void (*right*).

where Δ is the correction due to the shear term. This is to be compared with the distance in the FRW model given by Eq. (2.29). In the following analysis, we assume that the void is much smaller than the Hubble radius, and we define the small parameter η by

$$\eta \equiv a(t)r_v(t)/t, \quad (3.9)$$

i.e., the ratio of the radius of the void to the Hubble radius. We expand all the quantities in powers of η .

Now let us consider the jumps of θ and σ . The jump of the expansion given by Eq. (2.26) is calculated as

$$\theta'_1 = \theta_1 - \frac{4}{9}fk_1\gamma_1 \frac{(1 + v_1 \cos \Psi_1)^2 \eta_1}{v_1 + \cos \Psi_1 t_1}, \quad (3.10)$$

where we have defined the velocity and the γ -factor as

$$v_1 \equiv a(t_1) \frac{dr_1}{dt} = \beta \eta_1, \quad \gamma_1 \equiv (1 - v_1^2)^{-\frac{1}{2}}, \quad (3.11)$$

and the ratio of the shell mass to the “extracted” mass as

$$f \equiv \frac{4\pi D a^2 r_v^2}{(4\pi/3)a^3 r_v^3 \rho_{\text{FRW}}} \quad \text{with} \quad \rho_{\text{FRW}} = \frac{3H^2}{8\pi G}, \quad (3.12)$$

which will be set to unity, but at this stage we keep it as a free parameter for later discussion. We also used

$$u_a k^a = -k_1 \gamma_1 (1 + v_1 \cos \Psi_1), \quad n_c k^c = k_1 \gamma_1 (v_1 + \cos \Psi_1). \quad (3.13)$$

The shear induced by the shell is calculated using Eq.(2.27) as

$$\sigma'_{11} = -\sigma'_{22} = -\frac{2}{9}f \frac{k_1 \gamma_1 (1 - v_1^2) \sin^2 \Psi_1 \eta_1}{v_1 + \cos \Psi_1 t_1}, \quad (3.14)$$

where we have taken $e'_{2a} = (0, 0, 0, x'_1)$. Since the increase in the affine parameter during the travel through the void is given by

$$\lambda - \lambda_0 = \frac{t'_2 - t'_1}{k'_1} = 2 \frac{t_1}{k_1} \cos \Psi_1 \eta_1 + \mathcal{O}(\eta_1^2), \quad (3.15)$$

the correction term Δ in Eq. (3.8) is

$$|\Delta| \sim \sigma_1^{AB} \sigma_{AB1} (\lambda - \lambda_0)^2 = \frac{32}{81} f^2 \frac{(1 - v_1^2) \sin^4 \Psi_1 \cos^2 \Psi_1}{(v_1 + \cos \Psi_1)^2} \eta_1^4. \quad (3.16)$$

Thus the correction due to the shear is of order η_1^4 .

Now we study the modification of the redshift due to the existence of the void. The redshift is defined in the void model by

$$1 + z_V \equiv \frac{k_1}{k_2} \quad (3.17)$$

and in the FRW model by

$$1 + z_F \equiv \left(\frac{t_2}{t_1} \right)^{\frac{2}{3}}. \quad (3.18)$$

By a straightforward calculation, we find

$$\frac{1 + z_V}{1 + z_F} - 1 = \left(-\frac{16}{81} \cos^3 \Psi_1 + \frac{9}{8} \beta \cos \Psi_1 \right) \eta_1^3, \quad (3.19)$$

which agrees with the result of Thompson and Vishniac.¹³⁾ Thus, the leading order of the modification of redshift is order η_1^3 .

Next we study the modification of the angular-diameter distance. Expanding Eq. (3.8), we find

$$\begin{aligned} d_{AV}(t_2) &= d_{A1} + d_{A1} \frac{t_1}{k_1} \theta_1 \cos \Psi'_1 \eta_1 - d_{A1} \frac{4f}{9} \eta_1^2 \\ &\quad + d_{A1} \frac{t_1}{k_1} \theta_1 \left(\beta + \frac{2}{3} + \frac{2}{3} \cos^2 \Psi'_1 \right) \eta_1^2 + \mathcal{O}(\eta_1^3). \end{aligned} \quad (3.20)$$

For the FRW model, we find, from Eq. (2.29),

$$\begin{aligned} d_{AF}(t_2) &= d_{A1} + d_{A1} \frac{t_1}{k_1} \theta_1 \cos \Psi'_1 \eta_1 - \frac{4}{3} \cos^2 \Psi'_1 \eta_1^2 \\ &\quad + d_{A1} \frac{t_1}{k_1} \theta_1 \left(\beta + \frac{2}{3} + \frac{2}{3} \cos^2 \Psi'_1 \right) \eta_1^2 + \mathcal{O}(\eta_1^3). \end{aligned} \quad (3.21)$$

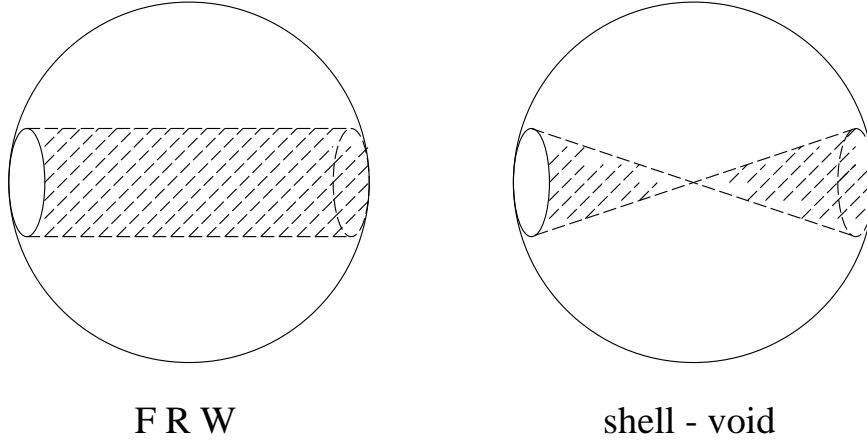


Fig. 3. Schematic picture for the volume of the matter which causes the Ricci focusing on the passing photon beam. In the FRW model (*left*), the beam is influenced by the matter contained inside the tube. In the void-shell system (*right*), the shell contains only the matter inside the cones.

Thus the difference reads

$$d_{\text{AV}}(t_2) - d_{\text{AF}}(t_2) = d_{\text{A1}} \left\{ \frac{4}{3} \cos^2 \Psi'_1 - \frac{4f}{9} \right\} \eta_1^2 + \mathcal{O}(\eta_1^3). \quad (3.22)$$

Let us focus on the leading term in the difference. When $\cos \Psi'_1$ is close to unity, i.e. when the beam passes near the center, the beam is de-magnified compared with the beam in the FRW model, to give a longer distance (we assumed $f = 1$). Contrastingly, when $\cos \Psi'_1$ is close to zero, i.e. when the impact parameter is large, the beam is magnified. One can also note that the leading term of $(d_{\text{AV}} - d_{\text{AF}})$ for $\cos \Psi'_1 = 1$ vanishes if $f = 3$. Recalling that f denotes the mass fraction of the dust shell to the mass that would have been in the void, we may say that in the void-shell system the Ricci focusing effect is weaker than in the FRW model by a factor of $\frac{1}{3}$. This can be explained in the following way (see Fig. 3). In the FRW universe, the beam suffers Ricci focusing by the matter within the tube shaded in the figure. On the other hand, in the void-shell system, the area of the shell which causes the Ricci focusing contains only the matter within the cones whose tops are at the center of the void. This explains the factor of $\frac{1}{3}$.

Our result disagrees with the result obtained by Sato,¹⁵⁾ who argued that the difference is of order η_1 . The disagreement comes from the junction condition for the distance at the time that the bundle crosses the shell. Sato assumed that the derivative of the distance with respect to the proper time measured by an observer at the boundary is continuous across the shell. However, we cannot read off any clear physical meaning that this condition should represent. Our condition, on the other hand, is obtained by integrating the Raychaudhuri equation, whose physical meaning is clear. As shown in the Appendix, the same result is obtained by a different method. Thus we conclude that the leading term in the difference is of order η_1^2 . In other words, when a light ray passes only one void during its travel from the source

to the observer, the modification of the distance compared with the whole distance is of order η_1^2 , which may be considered to be very small. However, this means that the *increase* in the distance during the time that the beam crosses one void is modified by the order of η_1 , since the radius of the void itself is of the order of η_1 . Moreover, the effect is cumulative when the beam passes through many voids successively. Thus, it is interesting to study a multi-void system. This is the subject of the next section.

3.2. Light propagation in multi-void system

In this section, we study the distance-redshift relation in a universe filled with voids. The simple model used here consists of randomly distributed voids, whose sizes evolve according to Eq. (3.4). *) We start from a point source at $t = t_1$ in the flat FRW universe. The light propagates in the FRW universe for a time interval $\sim 0.05 \times t_1$ and then enters the first void surrounded by a dust shell. When the ray bundle crosses the shell, we calculate the expansion and the null vector using the junction condition described in the previous sections. We perform the same calculation for the time that the light leaves the void. For simplicity, we assume that the light ray enters another shell as soon as it leaves one void (see Fig. 4). The entering angle (or impact parameter) is treated as a random variable. At each exiting moment, we can calculate the redshift z_V and the angular-diameter distance d_{AV} from the source. We continue until z_V exceeds a desired value. We also calculate the angular-diameter distance d_{AF} for a source at the same redshift in the FRW universe. By repeating this sequence of calculations, we accumulate a large number of data (typically $\sim 10^4$) for d_{AV}/d_{AF} . We omitted cases when the expansion θ becomes negative. The fraction is well below 1% even for the cases where the void size is about $0.1H_0^{-1}$, and thus it has no influence on the following discussion. We also neglect the shear effect in the subsequent calculations, since the effect is negligible, as we saw in the previous section.

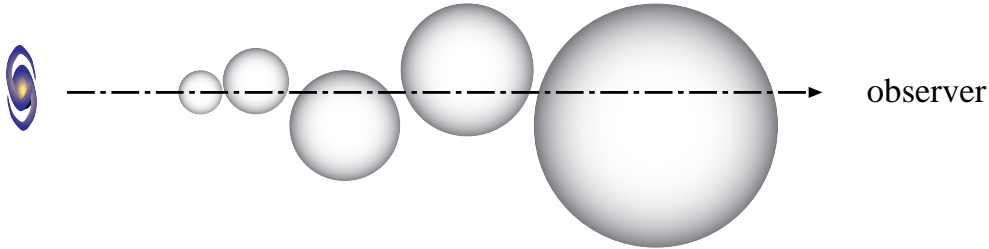


Fig. 4. Photon beam traveling through the universe filled with voids. We assume that the beam enters another void as soon as it leaves one void.

Figures. 5 and 6 display the probability distribution for d_{AV}/d_{AF} . In Fig. 5 we plot the distribution for samples at redshift between 1.0 and 1.1, and in Fig. 6 for samples at redshifts between 3.0 and 3.2. The sizes of the void are adjusted so that the void has evolved at the observed time to radii of (approximately) $0.01H_0^{-1}$, $0.05H_0^{-1}$ and $0.1H_0^{-1}$, where H_0^{-1} is the Horizon radius at the observed time. We

*) Our approach is similar to the method used by Holz and Wald.¹⁷⁾ We have just substituted a void-shell system for their particle-hole system.

can see that the distribution is peaked above unity by 2% (4%) when the void size is $0.01H^{-1}$ and by 4% (10%) when it is $0.05H^{-1}$ for $z \sim 1.0$ ($z \sim 3.0$), although the peak is rather broad for a large void size. The dispersion becomes even larger when the sample redshift is increased. Also note that the shape of the distribution is not symmetric.

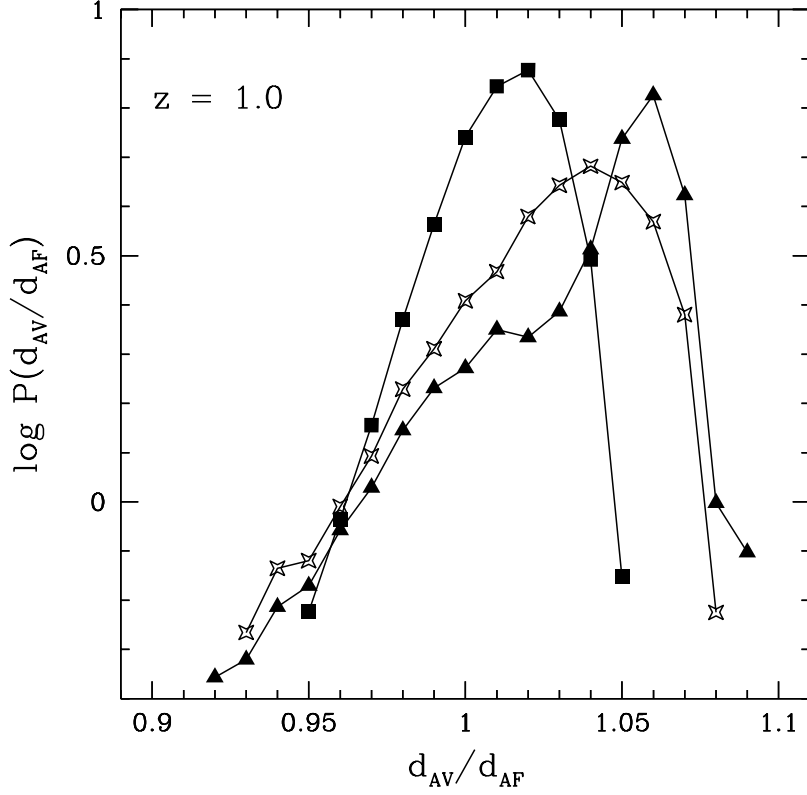


Fig. 5. Probability distribution P of d_{AV}/d_{AF} for samples at redshifts between 1.0 and 1.1. The normalization of P is such that the fraction of the beams which has d_{AV}/d_{AF} in the range $[x, x + dx]$ is given by $P(x)dx$. The radius of the void at present is $0.01H_0^{-1}$ (square), $0.05H_0^{-1}$ (cross), and $0.1H_0^{-1}$ (triangle) in each model.

When the void radius is $0.1H^{-1}$, the distribution seems to have a wavy feature. In order to see how this occurs, let us study higher order terms that we neglected in the previous section. Expanding Eq. (3-8) up to $\mathcal{O}(\eta_1^3)$, we find

$$\begin{aligned} \mathcal{O}(\eta_1^3) \text{ of } \frac{d_{AV}(t_2)}{d_0} = & -\frac{8}{9}f\left(\beta + \frac{2}{3}\right)\cos\Psi_1\eta_1^3 \\ & + \frac{t_1}{k_1}\frac{d_0'}{d_0}\left[\frac{8}{3}\cos^3\Psi_1 + \left(4\beta^2 + \frac{14}{3}\beta - \frac{8}{9}\right)\cos\Psi_1\right]\eta_1^3. \end{aligned} \quad (3-23)$$

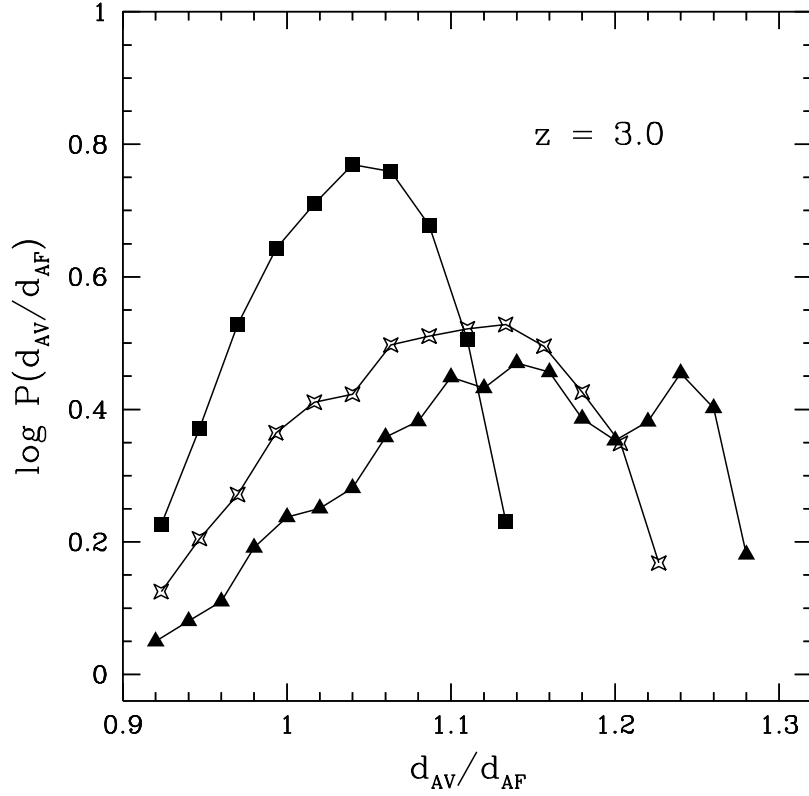


Fig. 6. Probability distribution of d_{AV}/d_{AF} for samples at redshifts between 3.0 and 3.2 . The normalization of P is the same with the previous figure. The size of the void is labeled by the same symbols as the previous figure.

For the FRW model, we find

$$\begin{aligned} \mathcal{O}(\eta_1^3) \text{ of } \frac{d_{AF}(t'_2)}{d_0} = & -\frac{8}{3} \left(\beta + \frac{2}{9} \cos^2 \Psi_1 \right) \cos \Psi_1 \eta_1^3 \\ & + \frac{t_1}{k_1} \frac{d'_0}{d_0} \left[\frac{40}{27} \cos^3 \Psi_1 + \left(4\beta^2 + \frac{14}{3}\beta - \frac{8}{9} \right) \cos \Psi_1 \right] \eta_1^3. \end{aligned} \quad (3.24)$$

Thus the difference reads

$$\begin{aligned} \frac{d_{AV}(t'_2) - d_{AF}(t'_2)}{d_0} = & \left(\frac{16}{27} + \frac{t_1}{k_1} \frac{d'_0}{d_0} \frac{32}{27} \right) \cos^3 \Psi_1 \eta_1^3 \\ & - \left[\frac{8}{9} (f - 3\beta) + \frac{16}{27} f \right] \cos \Psi_1 \eta_1^3. \end{aligned} \quad (3.25)$$

This factor takes a small negative value when $\cos \Psi_1$ is small, i.e. when the beams passes close to the void wall. It decreases (the absolute value increases) as the impact decreases, then at some point it starts to increase, and ends up with a slightly positive

value when $\cos\Psi_1 = 1$. This causes the wavy distributions, which can be seen more clearly for a larger size of the voids.

We find the peak of the distribution becomes close to unity when the void size is small. We can crudely interpretate this behavior as follows. While a light ray bundle passes one void, the distance is affected by the amount of $\sim \mathcal{O}(\eta^2)$. The number of the voids which the light ray passes through before it reaches the observer is $d_A/r_v \sim (1+z)/\eta$. Thus, the accumulation of the effects amounts to

$$\Delta d_A/d_{AF}(z) \sim (1+z)\eta. \quad (3\cdot 26)$$

This consideration seems reasonable judging from the figures.

Let us compare our model with the Swiss Cheese (SC) model. Light propagation in the SC model is studied using a similar approach by Holz and Wald.¹⁷⁾ According to their work, when the matter is condensed to point masses or compact objects, a large fraction of the beams from distant sources travel without being affected by the matter for most of their travel time. That is, a large fraction of the beams avoid the Ricci focusing effect, while a quite small fraction of the beams suffers strong shear focusing. Thus, the obtained distance for a fixed redshift favors a lower density model, even if the background model is a flat FRW model. On the other hand, in the void-shell system, a beam passes through a substantial fraction of the matter, resulting in a small difference from the FRW distance. In addition, when the beam successively passes through the voids, it is affected by almost the same amount of matter in the FRW universe as we have seen above. Thus, if the underdensity of the void is compensated by a surrounding (spherical) shell, the difference in distance from the FRW model is small. Also note that the distributions of distance are quite different for the SC model and the void model, reflecting the difference in the matter distribution. In principle, we can obtain information concerning the inhomogeneities from the scatter or distribution of the distance-redshift relation, though the current accuracy of observation is not sufficient to allow this.

We finally note the implications of our results on the determination of the cosmological parameters through the distance-redshift relation. As we have seen, the void structure increases the distance of a source compared with the distance in the FRW model; in this sense, the cosmological constant or a low density model is favored. However, the magnitude of the modification is about 2% for a void whose size is 1% of the horizon radius, which is well below the current error in the estimate of the absolute magnitude (or distance) of the standard candles, such as a type Ia super nova. The scatter around the peak is also well below the current error as long as the void is not too large ($< 1\%$ of the horizon radius).

§4. Summary

We have studied light propagation properties in a spherical void (empty region) embedded in a spatially flat FRW universe. The void is surrounded by an overdense wall, which we treated as a dust shell. We considered the null geodesic equation and the Raychaudhuri equation, and derived the junction condition for the expansion and the shear across the shell. Using these, the redshift and the distance were calculated

in the void-shell system, and we compared the results with the FRW relations. We have found that the modification of redshift by a single void is of order η^3 , and the modification of the distance is of order η^2 , where η is the ratio of the void size to the Hubble radius.

We have also discussed the cosmological implications of voids by considering a universe filled with voids. The void-filled universe slightly increases the mean distance and produces a dispersion in the distribution of the distance. This may work to lower the density parameter or favor the cosmological constant when the cosmological parameters are estimated through the distance-redshift relation of distant sources. However, for samples with redshifts ~ 1.0 , the magnitude of the effect is well below the current error in estimating the distance of the standard candles as long as the voids are within the observationally favored size.

Appendix A

— Simple Derivation of d_A for a Single Void —

Our analytic method based on the geometric optics equations (2.5) and (2.6) is not only useful for the present analysis but also can be extended to general spacetimes including singular hypersurfaces. For the model of a void in the flat FRW background, however, we have a simpler derivation of the angular-diameter distance which we now present.

Thompson and Vishniac derived not only the redshift deviation (3.19) but also the scattering angle of a photon:¹³⁾

$$\delta\alpha \equiv -\Psi_1 + \Psi'_1 + \Psi'_2 - \Psi_2 = \frac{4}{9}\eta_2^2 \sin(2\Psi_2). \quad (\text{A.1})$$

As depicted in Fig. 7, we define α as the angle formed between the direction of observation and the direction of the void's center, D_L as the comoving distance of the void's center, and D_S as the comoving distance of the light source. Hereafter the subscript S denotes a quantity at a light source. In the two-dimensional comoving space we denote each position by the vector symbol \mathbf{r} and introduce a vector basis, $[\mathbf{n}(\alpha), \mathbf{l}(\alpha)]$. The trajectory of a photon between a source and an observer was obtained in Ref. 14). It is given by

$$\begin{aligned} \mathbf{r}_S - \mathbf{r}_0 &= 3t_0 \left[(1 - \sqrt{a_S})\mathbf{n} + \left(1 - \sqrt{a_S} - \frac{D_L}{3t_0}\right) \delta\alpha \mathbf{l} \right] \\ &\equiv D_S \mathbf{n} + D_{LS} \delta\alpha \mathbf{l}, \end{aligned} \quad (\text{A.2})$$

where $D_{LS} \equiv D_S - D_L$. In the absence of a void, this relation reduces to

$$(\mathbf{r}_S - \mathbf{r}_0)_b = 3t_0(1 - \sqrt{a_S})\mathbf{n} \equiv D_S \mathbf{n}, \quad (\text{A.3})$$

where the subscript b denotes a background unperturbed quantity.

The angular-diameter distance of a light source is originally defined as

$$d_A \equiv \frac{\mathcal{D}}{\delta}, \quad (\text{A.4})$$

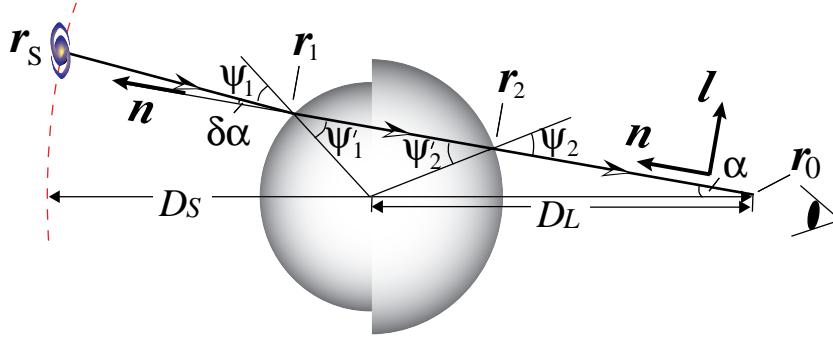


Fig. 7. Cross section of a void on the $\varphi = \pi/2$ plane of the model. We depict the trajectory of a photon from a light source to an observer. Define α as the angle formed between the direction of observation and the direction of the void's center, $\delta\alpha$ as the scattering angle of a photon, D_L as the comoving distance of the void's center, and D_S as the comoving distance of the light source. We denote each position by a vector symbol \mathbf{r} , and introduce a vector basis, $\{\mathbf{n}(\alpha), \mathbf{l}(\alpha)\}$, in the two-dimensional comoving space.

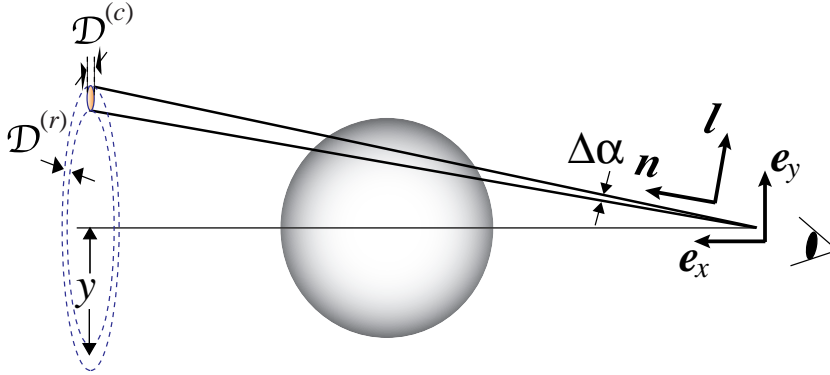


Fig. 8. Schematic picture of a null geodesic congruence. $\mathcal{D}^{(r)}$ and $\mathcal{D}^{(c)}$ denote, respectively, the radial component and the circumferential component of the proper distance at a source for a fixed angular diameter.

where \mathcal{D} is the proper distance across the source and δ is its angular diameter. Here we calculate the manner in which \mathcal{D} is changed by a void for a fixed δ , considering the radial direction from the void's center and the circumferential direction separately (see Fig. 8). The radial component $\mathcal{D}^{(r)}$ and the circumferential component $\mathcal{D}^{(c)}$ are written as

$$\mathcal{D}^{(r)} = \left| \frac{d(\mathbf{r}_S - \mathbf{r}_0)}{d\alpha} \right| \Delta\alpha, \quad (\text{A}\cdot 5)$$

$$\mathcal{D}^{(c)} \propto y = (\mathbf{r}_S - \mathbf{r}_0) \cdot \mathbf{e}_y, \quad (\text{A}\cdot 6)$$

where y , \mathbf{e}_y and $\Delta\alpha$ are defined in Fig. 8. A straightforward calculation leads to

$$\frac{\Delta d_A^{(r)}}{d_A^{(r)}} = \frac{\mathcal{D}^{(r)}}{\mathcal{D}_b^{(r)}} - 1 = \frac{D_{LS}}{D_S} \frac{d(\delta\alpha)}{d\alpha}, \quad (\text{A}\cdot 7)$$

$$\frac{\Delta d_A^{(c)}}{d_A^{(c)}} = \frac{\mathcal{D}^{(c)}}{\mathcal{D}_b^{(c)}} - 1 = \frac{D_{LS}}{D_S} \delta\alpha \cot \alpha. \quad (\text{A}\cdot 8)$$

Thus, the order of magnitude of the modification of the distance is essentially determined by the scattering angle $\delta\alpha$, which is of order η_2^2 .

Acknowledgements

The authors thank Kouji Nakamura of Keio University for valuable discussions. N. Sugiura, D. Ida and N. Sakai are supported by research fellowships of the Japan Society for the Promotion of Science for Young Scientists.

References

- [1] R. P. Kirshner, A. Oemler, Jr., P. L. Schechter and S. A. Sackett, *Astrophys. J.* **248** (1981), L57.
- [2] R. P. Kirshner, A. Oemler, Jr., P. L. Schechter and S. A. Sackett, *Astrophys. J.* **314** (1987), 493.
- [3] V. de Lapparent, M. J. Geller and J. P. Huchra, *Astrophys. J.* **302** (1986), L1.
- [4] M. J. Geller and J. P. Huchra, *Science* **246** (1989), 897.
- [5] L. N. da Costa, et. al., *Astrophys. J.* **424** (1996), L1.
- [6] H. El-Ad, T. Piran and L. N. da Costa, *Astrophys. J.* **462** (1996), L13,
H. El-Ad, T. Piran and L. N. da Costa, *Mon. Not. R. Astron. Soc.* **287** (1997), 790,
H. El-Ad and T. Piran, *Astrophys. J.* **491** (1997), 421.
- [7] P. J. E. Peebles, *Astrophys. J.* **257** (1982), 438,
Y. Hoffman and J. Shaham, *ibid* **262** (1982), L23.
- [8] H. Sato, *Prog. Theor. Phys.* **68** (1982), 236.
H. Sato and K. Maeda, *Prog. Theor. Phys.* **70** (1983), 119.
- [9] K. Maeda and H. Sato, *Prog. Theor. Phys.* **70** (1983), 772, **70** (1983), 1276.
- [10] W. Israel, *Nuovo Cim.* **44B** (1966), 1.
- [11] J. P. Ostriker and L. N. Cowie, *Astrophys. J.* **243** (1981), L127,
S. Ikeuchi, *Publ. Astron. Soc. Japan* **333** (1981), 211.
- [12] L. Amendola, C. Baccigalupi, R. Konoplick, F. Occhionero and S. Rubin, *Phys. Rev.* **D54** (1996), 7199.
- [13] K. L. Thompson and E. T. Vishniac, *Astrophys. J.* **313** (1987), 517.
- [14] N. Sakai, N. Sugiyama and J. Yokoyama, *Astrophys. J.* **510** (1999), 1.
- [15] H. Sato, *Prog. Theor. Phys.* **73** (1985), 649.
- [16] C. C. Dyer and R. C. Roeder, *Astrophys. J.* **174** (1972), L115.
- [17] D. Holz and R. Wald, *Phys. Rev.* **D58** (1998), 063501.
- [18] R. Wald, *General Relativity* (The University of Chicago Press, Chicago, 1984).
- [19] M. Sasaki, *Prog. Theor. Phys.* **90** (1993), 753.
- [20] R. K. Sachs, *Proc. R. Soc. London* **A264** (1961), 309.
- [21] E. Bertschinger, *Astrophys. J. S.* **58** (1985), 1.